Ab initio and RRKM study of the HCN/HNC elimination channels from vinyl cyanide

ARTICLE *in* THE JOURNAL OF PHYSICAL CHEMISTRY A · FEBRUARY 2011

Impact Factor: 2.69 · DOI: 10.1021/jp109843a · Source: PubMed

THE JOURNAL OF PHYSICAL CHEMISTRY A

ARTICLE

pubs.acs.org/JPCA

Ab Initio and RRKM Study of the HCN/HNC Elimination Channels from Vinyl Cyanide

Zahra Homayoon,[†,‡] Saulo A. Vázquez,[†] Roberto Rodríguez-Fernández,[†] and Emilio Martínez-Núñez*[,†]

[†]Departamento de Química Física y Centro Singular de Investigación en Química Biológica y Materiales Moleculares, Campus Vida, Universidad de Santiago de Compostela, 15782 Santiago de Compostela, Spain

[‡]Department of Chemistry, College of Sciences, Shiraz University, Shiraz 71454, Iran

Supporting Information

ABSTRACT: Ab initio CCSD and CCSD(T) calculations with the 6-311+G(2d,2p) and the 6-311++G(3df,3pd) basis sets were carried out to characterize the vinyl cyanide (C_3H_3N) dissociation channels leading to hydrogen cyanide (HCN) and its isomer hydrogen isocyanide (HNC). Our computations predict three elimination channels giving rise to HCN and another four channels leading to HNC formation. The relative HCN/HNC branching ratios as a function of internal energy of vinyl cyanide were computed using RRKM theory and the kinetic Monte Carlo method. At low internal energies (120 kcal/mol), the total HCN/HNC ratio is about 14, but at 148 kcal/mol (193 nm) this ratio becomes 1.9, in contrast with the value 124 obtained in a previous ab initio/RRKM study at 193 nm (Derecskei-Kovacs, A.; North, S. W. *J. Chem. Phys.* **1999**, *110*, 2862). Moreover, our theoretical results predict a ratio of rovibrationally excited acetylene over total acetylene of 3.3, in perfect agreement with very recent experimental measurements (Wilhelm, M. J.; Nikow, M.; Letendre, L.; Dai, H.-L. *J. Chem. Phys.* **2009**, *130*, 044307).

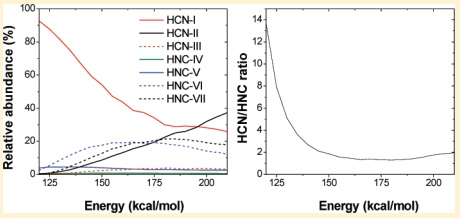

INTRODUCTION

The eliminations of hydrogen halides (HX, X = F, Cl, and Br) in photofragmentations of haloethylenes have been the subject of numerous theoretical and experimental studies.[1−25] Photoexcitation of these compounds at 193 nm leads to several competing channels for HX formation. HX eliminations may proceed via either three-centered or four-centered transition states. The analysis of the product energy partitioning in the photodissociation of haloethylenes indicates that HX eliminations take place on the ground electronic state potential energy surface (PES) after internal conversion from the electronic excited state[11,13,14,17,18]

The photodissociation of the more complex vinyl cyanide (VC) chemical species has also been studied recently.[26−32] Like for the haloethylenes, VC exhibits radical and molecular elimination channels when it is photoexcited at 193 nm. Fahr and Laufer[29] suggested that the formation of triplet vinylidene ($:CCH_2$) and HCN is a dominant channel in the photodissociation of the molecule at 190 nm using time-resolved UV absorption spectroscopy. Blank et al.,[26] later on, suggested that all dissociation channels occur on the ground electronic state S_0 after internal conversion from the electronically excited S_1 state. The reaction mechanism leading to triplet vinylidene and HCN was ruled out based on energy conservation arguments.[26] In a more recent study, Wilhelm et al.[32] rendered further support to the exclusion of the triplet vinylidene + HCN reaction path, using time-resolved Fourier transform infrared emission spectroscopy (TR-FTIRES).

Derecskei-Kovacs and North[30] performed ab initio calculations of the dissociation channels of vinyl cyanide and found two different pathways for HCN formation. The first one proceeds via a three-centered (3C) transition state forming singlet vinylidene and hydrogen cyanide (HCN), and the second one proceeds via a four-centered (4C) transition state giving rise to acetylene (HCCH) and hydrogen isocyanide (HNC) as coproduct. According to their RRKM calculations, the 3C process is 124 times faster than the 4C process for an energy corresponding to a photon wavelength of 193 nm. This means that, according to the HCN(HNC) reaction paths described above, the HCN/HNC ratio would be 124; i.e., HNC formation is negligible. Later on Letendre and Dai,[31] using the TR-FTIRES technique, found significant IR emission from acetylene and HNC, which is in contradiction with the ab initio results of Derecskei-Kovacs and North.[30] However, the relative importance of the HCN and HNC reaction mechanisms was not determined in the experimental study.

In the most recent experimental study on the photodissociation of VC and perdeuterovinyl cyanide at 193 nm, Wilhelm et al.[32] were able to discern the relative abundance of the HCN and HNC products. They deduced the HCN/HNC ratio assuming that the ab initio calculations of Derecskei-Kovacs and North[30] mentioned above were correct. In particular they assumed that HCN is formed alongside vinylidene and HNC is formed with

Received: October 14, 2010
Published: January 25, 2011

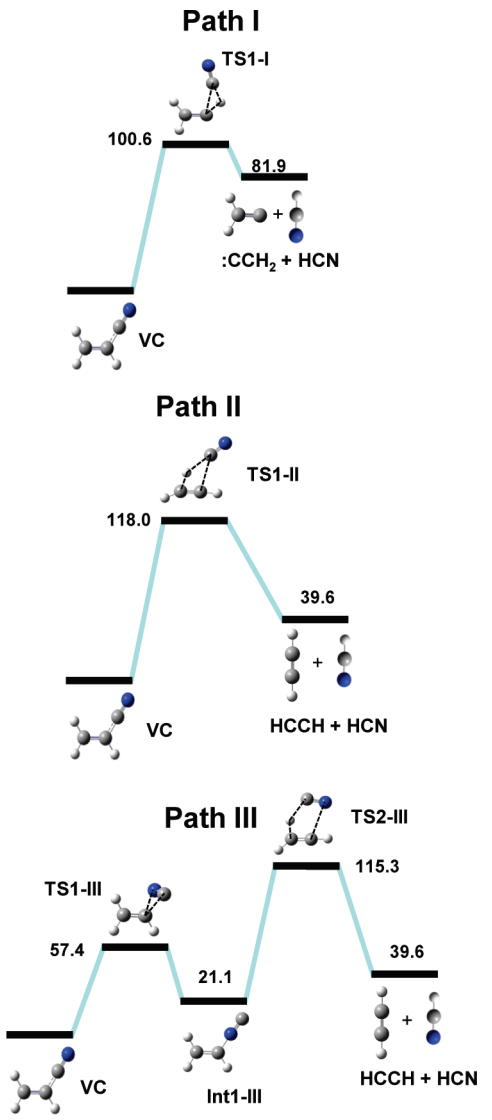

Figure 1. Schematic potential energy diagram for paths I−III (leading to HCN formation). The values are the relative energies (in kcal/mol).

acetylene. Additionally, if vinylidene is formed as a coproduct of HCN, the rapid vinylidene−acetylene isomerization process will lead to highly rovibrationally excited acetylene, since the process is very exothermic.[4] When acetylene is formed as a coproduct of HNC, no isomerization takes place and its rovibrational energy distribution will be colder. Following these arguments and their measured ratio of excited acetylene to total acetylene formation (0.77), they obtained a value for the HCN/HNC branching ratio of 3.3 (0.77/0.23). Wilhelm et al.[32] claimed that the ab initio calculations of the transition states for the HCN and HNC formation processes should be re-examined since the RRKM branching ratio calculated in the ab initio study is 124,[30] in sharp contrast to their experimentally determined value of 3.3. In particular, Wilhelm et al.[32] suggest that the 4C transition state should be ∼10.5 kcal/mol below the 3C transition state to reconcile theory with experiment. However, the previous ab initio study predicts the 4C transition state to lie ∼9 kcal/mol above the 3C transition state.[30] In our opinion, it seems more plausible that new HCN(HNC) reaction paths, not found in the previous ab initio study,[30] may contribute significantly to the formation of HCN or its isomer HNC.

In this paper further electronic structure calculations were performed to characterize the relevant regions of the ground state potential energy surface (PES) associated with the HCN and HNC eliminations from vinyl cyanide (VC). Microcanonical $k(E)$ rate constants were also computed as a function of the internal energy of VC using RRKM theory. With the calculated $k(E)$ and modeling the kinetics using a Monte Carlo technique, the HCN and HNC product abundances were evaluated for the different reaction paths and compared with the recent experimental results of Wilhelm et al.[32]

I. COMPUTATIONAL DETAILS

A. Electronic Structure Calculations. Ab initio calculations were carried out to model the ground state potential energy surface (PES) of the HCN and HNC elimination channels from vinyl cyanide. The calculations involve CCSD/6-311+G(2d,2p) optimizations and frequency analyses to characterize the stationary points as minima or saddle points and to evaluate zero-point vibrational energies (ZPE). The minimum energy path (MEP)[33] was followed at the MP2/6-31+G(d,p) level of theory to make sure that a transition structure connects with the expected minima.

In order to obtain accurate energies, we also performed CCSD(T)/6-311++G(3df,3pd) single-point calculations at the CCSD/6-311+G(2d,2p) optimized geometries [these calculations are referred as CCSD(T)/6-311++G(3df,3pd)//CCSD/6-311+G(2d,2p)].

The Gaussian 09 program package[34] was employed for all the electronic structure calculations.

B. Kinetic Calculations. In this study, the following elementary steps associated with the elimination of HCN (paths I−III) and HNC (paths IV−VII) were taken into account (see also Figures 1 and 2):

path I

$$\mathrm{VC} \xrightarrow{k_1} :\mathrm{CCH_2} + \mathrm{HCN} \quad (1)$$

path II

$$\mathrm{VC} \xrightarrow{k_2} \mathrm{HCCH} + \mathrm{HCN} \quad (2)$$

path III

$$\mathrm{VC} \underset{k_3}{\overset{k_4}{\leftrightarrow}} \mathrm{Int1\text{-}III} \quad (3)$$

$$\mathrm{Int1\text{-}III} \xrightarrow{k_5} \mathrm{HCCH} + \mathrm{HCN} \quad (4)$$

path IV

$$\mathrm{VC} \underset{k_6}{\overset{k_7}{\leftrightarrow}} \mathrm{Int1\text{-}IV} \quad (5)$$

$$\mathrm{Int1\text{-}IV} \xrightarrow{k_8} \mathrm{HCCH} + \mathrm{HNC} \quad (6)$$

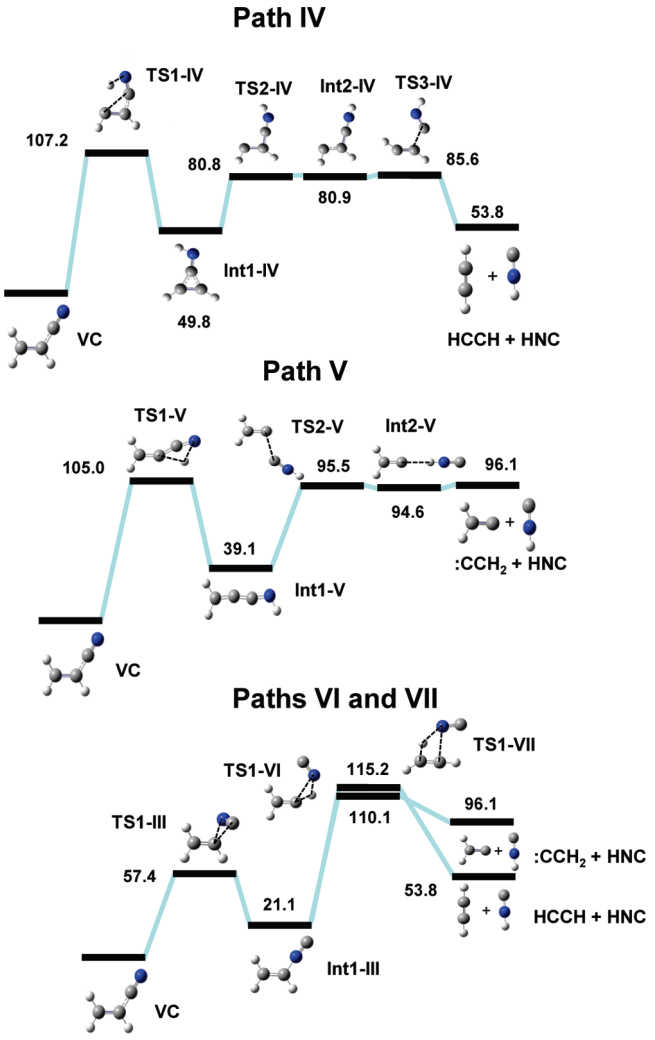

Figure 2. Schematic potential energy diagram for paths IV−VII (leading to HNC formation). The values are the relative energies (in kcal/mol).

path V

$$\mathrm{VC} \underset{k_9}{\overset{k_{10}}{\leftrightarrow}} \mathrm{Int1\text{-}V} \tag{7}$$

$$\mathrm{Int1\text{-}V} \xrightarrow{k_{11}} :\mathrm{CCH_2} + \mathrm{HNC} \tag{8}$$

path VI

$$\mathrm{Int1\text{-}III} \xrightarrow{k_{12}} :\mathrm{CCH_2} + \mathrm{HNC} \tag{9}$$

path VII

$$\mathrm{Int1\text{-}III} \xrightarrow{k_{13}} \mathrm{HCCH} + \mathrm{HNC} \tag{10}$$

Rate coefficients $k_8(E)$ were calculated assuming that Int1-IV is connected to the products via TS3-IV, since the energy of Int2-IV, after adding the zero-point energies, is above that of TS2-IV (see Figure 2). Additionally, for the rate coefficients $k_{11}(E)$, the assumption is that once TS2-V is overcome, vinylidene and HNC are obtained. Both assumptions seem reasonable, but nevertheless, as will be seen below, the contribution of paths IV and V to the formation of HNC and HCN is negligible in the whole range of energies studied here, in comparison with the others paths.

The microcanonical rate coefficients $k_i(E)$ (with i = 1−13) were calculated using RRKM theory[35]

$$k_i(E) = \sigma \frac{\sum_n P_i(E - \varepsilon_n^{\mathrm{ts},\,i})}{h\rho_i(E)} \tag{11}$$

where σ is the reaction path degeneracy, $\rho_i(E)$ is the density of states at the reactant, $P_i(E)$ is the one-dimensional tunneling probability as a function of energy E, and $\varepsilon_n^{\mathrm{ts},i}$ are the vibrational energy levels of the transition state for elementary step i. In the classical limit of no tunneling, the numerator of eq 11 tends to the total number of states at the transition state with energy less than or equal to E. A generalized Eckart potential was used to calculate $P_i(E)$, and the density of states was evaluated by direct count of the harmonic vibrational states using the Beyer−Swinehart algorithm. The CCSD(T)/6-311++G(3df,3pd)//CCSD/6-311+G(2d,2p) energies and the CCSD/6-311+G(2d,2p) frequencies were employed for these calculations. The vibrational frequencies for all the stationary states are collected in Table 1 of the Supporting Information.

The method used here to model the time evolution of reactants, intermediates, and products is kinetic Monte Carlo (KMC).[36,37] KMC is a very useful Monte Carlo simulation for modeling the transient behavior of various molecular species that participate in many highly coupled chemical reactions. The method is an alternative to the traditional procedure of numerically solving the deterministic reaction rate equations.

To calculate the populations of all the species involved in the photodissociation of VC as a function of time, the above reaction paths were considered and the RRKM rates calculated as above were employed. To obtain an average value of these populations, 10 KMC runs were performed for each internal energy of VC with the same initial conditions. Each of the 10 KMC runs differ in the random number seed used in the stochastic procedure. Using a higher number of KMC runs for each energy does not change the branching ratios obtained in this study.

II. RESULTS AND DISCUSSION

A. Electronic Structure Calculations. The different paths found in our electronic structure calculations for the HCN and HNC eliminations from VC are shown graphically in Figures 1 and 2, which include relative energies and zero-point energy contributions. A total of three HCN elimination channels (paths I−III in Figure 1) and four HNC elimination channels (paths IV−VII in Figure 2) were found in this study. The geometries of all the stationary points found in this study are collected in Table 2 of the Supporting Information.

Path I proceeds via a three-centered transition state (TS1-I) and is the same as that found by Derecskei-Kovacs and North[30] (see Figure 3 of their paper) in their ab initio study. The energies of the stationary points found in our study agree very well with their QCISD(T)/6-311++G(d,p)//MP2/6-31G(d,p) calculations.[30] In particular, TS1-I lies 100.6 kcal/mol above VC according to our CCSD(T)/6-311++G(3df,3pd)//CCSD/6-311+G(2d,2p) calculations, in comparison with 100.8 kcal/mol, found by Derecskei-Kovacs and North (their transition state structure is called A2 in Figure 3 of their paper).[30]

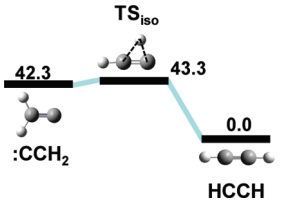

Figure 3. Schematic potential energy diagram for the vinylidene−acetylene isomerization process. The values are the relative energies (in kcal/mol).

Figure 3 shows the path connecting vinylidene (:CCH_2) and acetylene (HCCH). The CCSD(T)/6-311++G(3df,3pd)//CCSD/6-311+G(2d,2p) calculations predict an isomerization transition state that lies only 1 kcal/mol above vinylidene, suggesting a rapid isomerization process. In a previous chemical dynamics simulation study, conducted in our research group, a lifetime of only 37 fs was found for vinilydene.[4] This value is in agreement with that estimated by Ervin et al.,[38] 40−200 fs, based on negative ion photodetachment spectral line widths. Considering the vinylidene−acetylene potential energy profile, it was also suggested that part of the reverse isomerization barrier (of 43.3 kcal/mol) may be released as translational energy of the fragments in the photodissociation of vinyl chloride.[13] This suggestion was confirmed in our previous chemical dynamics study, and the snapshots of the trajectories showed a concerted mechanism with isomerization (of vinylidene to acetylene) and (HCl) elimination occurring at the same time in the dissociation of vinyl chloride.[4] A similar mechanism was invoked by Blank et al.[26] to explain the product energy partitioning found in the photodissociation of vinyl cyanide at 193 nm.

The other two paths that generate HCN (II and III in Figure 1) were not found in the previous ab initio study.[30] Path II proceeds via a four-centered planar transition state (TS1-II) that lies 118.0 kcal/mol above VC. HCN is produced with acetylene (instead of vinylidene) as coproduct. Path III first involves the isomerization of vinyl cyanide to vinyl isocyanide (Int1-III).[39] Then, vinyl isocyanide gives rise to HCN and acetylene, a process that goes through a five-centered transition state (TS2-III). The energy of this transition state is 115.3 kcal/mol with respect to VC.

Paths IV−VII in Figure 2 form hydrogen isocyanide (HNC). Path IV proceeds via a planar three-centered transition state (TS1-IV), which is the same as transition state A1 in the previous ab initio study.[30] They refer to this path as a four-centered mechanism, because they claim it connects the reactant with acetylene and HNC directly (see Figure 4 of their paper).[30] However, MEP calculations performed here show that TS1-IV actually connects the reactant with cycloprop-2-enimine (int1-IV in Figure 2), which lies 49.8 kcal/mol above the reactant. Cycloprop-2-enimine can give rise to acetylene and hydrogen isocyanide (HNC) after isomerizing via the unstable intermediate Int2-IV. The energy of TS1-IV is 107.2 kcal/mol with respect to VC, in comparison with the 109.6 kcal/mol found in the previous ab initio study.[30]

Three more mechanisms that form HNC have been identified in this study. Path V proceeds through allen-1-imine (Int1-IV), an intermediate formed after H transfer between the C and N atoms of VC. The H transfer transition state TS1-V is planar and lies 105.0 kcal/mol above VC. Allen-1-imine can react back to the reactant or dissociate to vinylidene and HNC via the van der Waals minimum Int2-V.

Table 1. Final Relative Populations of HCN and HNC Obtained in Channels I−VII

	HCN			HNC				HCN/HNC
E^a	I	II	III	IV	V	VI	VII	
120	92.7	0.5	0.1	0.4	3.8	2.4	0.1	13.7
148	55.3	8.2	2.2	0.7	4.0	17.6	12.0	1.9
200	28.1	31.8	3.6	0.6	2.6	14.1	19.2	1.7

[a]Energy in kcal/mol.

Paths VI and VII share the first part (the isomerization of VC to vinyl isocyanide) with path III. Vinyl isocyanide (Int1-III) can dissociate via either three-centered or four-centered planar transition states giving rise to vinylidene + HNC (channel VI) and acetylene + HNC (channel VII), respectively (see Figure 2). The energies of these two transition states are 110.1 and 115.2 kcal/mol with respect to the global minimum (VC), respectively. These two transition states resemble the corresponding three-centered and four-centered transition states from VC (TS1-I and TS1-II). The main difference is the HCN(HNC) isomer formed in each process; TS1-I and TS1-II form HCN, whereas TS1-VI and TS1-VII form HNC. The energies of the three-centered transition states (TS1-I and TS1-VI) are 5−7 kcal/mol lower than those of the corresponding four-centered transition states (TS1-II and TS1-VII). As will be seen below, the three-centered and four-centered mechanisms from VC (paths I and II) and vinyl isocyanide (paths VI and VII) are major channels for the HCN and HNC formation, respectively.

B. Kinetics Calculations. As indicated above, the population of the various species involved in paths I−VII can be modeled using combined RRKM and KMC calculations. The RRKM calculations are used for the rate coefficients and the KMC ones for the relative population of all the molecular species. In particular, we are interested in the $t \rightarrow \infty$ HCN and HNC relative populations for different VC internal energies. Figure 4 shows these populations as a function of time and reaction path for three different energies: 120, 148, and 200 kcal/mol. The energy of 148 kcal/mol corresponds to a photon wavelength of 193 nm and was selected to compare with the experimental results of Wilhelm et al.[32]

At the lowest energy of 120 kcal/mol, path I is, by far, the most important one, and HCN is formed via this mechanism with a probability of 93% (see also Table 1). Paths II and III contribute to the HCN abundance only 0.6%. The total HNC yield amounts to 6.3%, with path V being slightly favored over the other HNC paths. The total HCN/HNC branching ratio, which reaches a constant value after 300 ns (see Figure 4), is 13.7 at this energy.

At 148 kcal/mol (193 nm), the percentage of HCN formed via path I decreases to 55%, with respect to the 93% calculated at 120 kcal/mol. At this energy HCN is also formed significantly via the four-centered mechanism II (8.2%) and to a less extent via path III (2.2%). HNC is formed primarily through paths VI (17.6%) and VII (12.0%). The fact that paths VI and VII, which proceed via relatively high-energy transition states, become increasingly important as the internal energy increases is due to the presence of very low vibrational frequencies for the associated transition states (TS1-VI and TS1-VII; see Table 1 of the Supporting Information) that makes these processes entropically more favorable. The total HCN/HNC branching ratio at 193 nm obtained in our study decreases (with respect to the value at 120 kcal/mol) to 1.9, supporting the recent experimental papers

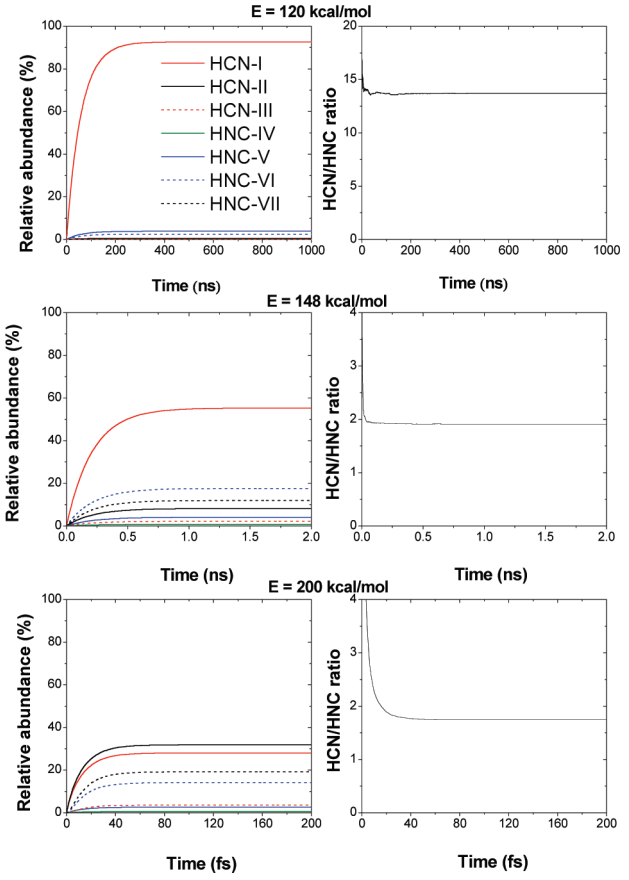

Figure 4. Populations, as a function of time, of HCN and HNC obtained in paths I−VII for three different energies and total HCN/HNC ratio.

of Dai and co-workers[31,32] that the relative presence of HNC is more important than expected from the previous ab initio calculations.[30] This point will be discussed in more detail below.

At the highest energy considered in this study (200 kcal/mol), HCN formation via the four-centered mechanism (path II) becomes the dominant channel with a percentage of 32% vs 28% obtained for the three-centered mechanism (path I). As discussed above, the increasing importance of path II with internal energy can be understood in terms of entropic effects. As the energy increases the entropic factor becomes more important than the relative magnitude of the energy barriers (enthalpic factor). The presence of low vibrational frequencies in TS1-II makes the numerator of eq 11 increase more rapidly with energy for path II than for path I. Again this entropic factor explains why HNC produced via path VII is more important at the highest energy than that produced via path VI, even though the corresponding transition state for path VII is 5 kcal/mol higher in energy than that for path VI.

Finally, the relative abundance of the HCN and HNC isomers produced in each path is depicted graphically in Figure 5 for a range of internal energies. For all energies except the lowest ones, only paths I, II, VI, and VII contribute significantly to the abundance of HNC and HCN isomers. As seen in the figure, the three-centered HCN formation mechanism (path I) dominates up to an energy of 195 kcal/mol. For higher energies, the four-centered mechanism (path II) is the major one. In the whole range of energies, the HCN abundance is always greater than the

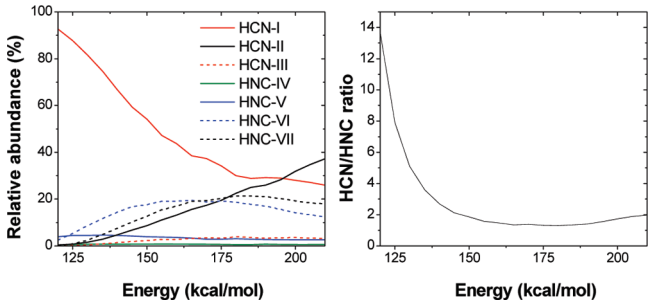

Figure 5. Final populations of HCN and HNC obtained for paths I−VII and total HCN/HNC ratio as a function of energy.

HNC abundance; the HCN/HNC ratio, however, shows a minimum value of 1.3 at 180 kcal/mol. This minimum ratio coincides with the maximum in the curve for the HNC abundance produced in channel VII. At this energy the relative importance of paths I, II, VI, and VII is 1, 0.75, 0.62 and 0.71, respectively. These results indicate that the dissociation channels that produce HNC are major dissociation channels that compete with those that generate HCN. This results is in agreement with the most recent experimental results.[32]

C. Comparison with Experiment. The HCN/HNC branching ratio calculated by Derecskei-Kovacs and North[30] at 148 kcal/mol (193 nm) was 124. As mentioned above, the previous ab initio results are incorrect since what they call four-centered dissociation (Figure 4 of their paper[30] or TS1-IV in this paper) does not actually connect vinyl cyanide with acetylene and HNC; this path is more complex and involves the intermediate cyclo-prop-2-enimine, as explained above. Nevertheless, taking only paths I and IV into account, as the previous ab initio study predicted,[30] the HCN/HNC branching ratio, calculated with our computed paths and frequencies, would be 79. This value is lower than that obtained using by Derecskei-Kovacs and North[30] of 124 because the corresponding transition state (TS1-IV in our paper and A1 in their paper) is 2.4 kcal/mol higher in energy in their calculations compared to our results and also because path IV is different in their study. In any case, paths I and IV alone are not enough to explain the experimental results of Wilhelm et al.[32] as they claim in their paper. Taking into account all the channels found in our study, the computed HCN/HNC branching ratio is 1.9 at 193 nm. This value is much smaller than 124 (or 79) and tells us about the importance of the new channels found in this study. Moreover, as detailed below, our computed paths and kinetic results are in perfect agreement with the recent experimental data of Wilhelm et al.[32]

Wilhelm et al.[32] estimated the HCN/HNC branching ratio indirectly. They measured the ratio of highly rovibrationally excited acetylene population to the total acetylene population formed as a function of time in the photodissociation of vinyl cyanide at 193 nm. Analyzing their time-resolved infrared spectra, they obtained a value of 0.77 for the nascent population ratio of excited/total acetylene molecules. This means that the ratio of rovibrationally excited acetylene to minimally excited acetylene is 0.77/0.23 = 3.3. To interpret this value, they suggest that highly excited acetylene comes from vinylidene, since the vinylidene−acetylene isomerization process adds an additional 42.3 kcal/mol (see Figure 3) of internal excitation on top of any energy originally partitioned to vinylidene. In addition, the fraction of minimally excited acetylene is formed directly in the photodissociation of vinyl cyanide as one of the photofrag-

ments.[32] In addition, based on the two mechanisms proposed in the ab initio study of Derecskei-Kovacs and North,[30] Wilhelm et al.[32] regarded the total population of vinylidene as the HCN population, since these are the two photofragments of the 3C process from VC (path I here and see also Figure 3 of ref 30), whereas acetylene is formed directly (without a previous isomerization) alongside HNC according to Figure 4 of ref 30 Therefore, they equated the population of highly rovibrationally excited acetylene (or vinylidene) to that of HCN and the population of minimally rovibrationally excited acetylene to that of HNC, determining a HCN/HNC ratio of 3.3.

As indicated above, the present ab initio calculations show that HCN may be formed either with vinylidene as coproduct (path I) or with acetylene as coproduct (paths II and III). Moreover, HNC can be formed as well alongside acetylene (paths IV and VII) or vinylidene (paths V and VI). Assuming, as Wilhelm et al.[32] did, that rovibrationally excited acetylene comes from vinylidene and that the population of rovibrationally unexcited acetylene is a consequence of the direct formation of this molecule, one can recalculate theoretically, using our ab initio and kinetic modeling results, the vinylidene/acetylene ratio to compare with that measured by Wilhelm et al.[32] Using the populations of Table 1 at 148 kcal/mol, the vinylidene/acetylene ratio (calculated as the sum of the populations of paths I, V, and VI divided by the populations of paths II, III, IV, and VII) is 3.3, in perfect agreement with the experimental measured value of Wilhelm et al.[32]

III. CONCLUSIONS

The ab initio calculations performed in this work provide seven channels for HCN(HNC) elimination from vinyl cyanide, five of which are new; previous ab initio calculations found only two channels. Three of these new paths are extremely important to explain the experimentally observed HCN/HNC branching ratios. Among the new paths found here the major ones to generate HCN or HNC are

i. A four-centered transition state that leads to acetylene and hydrogen cyanide (path II).
ii. Paths VI and VII that involve, as a first step, the isomerization of vinyl cyanide to vinyl isocyanide.

Then, from vinyl isocyanide there is a three-centered mechanism leading to vinylidene and hydrogen isocyanide (path VI) and a four-centered mechanism leading to acetylene and hydrogen cyanide (path VII).

Additionally, one of the paths reported in a previous ab initio study[30] was found to be wrong, since the transition state does not really connect the expected chemical species (VC and HCCH + HNC). This path (IV in our study) proceeds via cycloprop-2-enimine and is more complex, as it involves more steps than previously thought. This path was found to be unimportant to calculate the HCN/HNC branching ratios. The remaining two paths are also not very important and involve isomerizations of VC to vinyl isocyanide (path III) and allen-1-imine (path V).

With this new ab initio picture of the HCN(HNC) elimination channels, the HCN/HNC branching ratios were calculated from the RRKM rate coefficients and KMC simulations. The predicted HCN/HNC branching ratio at 193 nm is 1.9, which differs markedly from the previous theoretical value of 124. Moreover, the theoretical calculations of the present work also explain the recently measured value for the ratio of rovibrationally excited acetylene to total acetylene in the photodissociation of vinyl cyanide at 193 nm. The value obtained experimentally is 3.3, in perfect agreement with that calculated in this work using our ab initio/RRKM/KMC results.

■ ASSOCIATED CONTENT

Supporting Information. Vibrational frequencies and geometries of all stationary points. This material is available free of charge via the Internet at http://pubs.acs.org.

■ AUTHOR INFORMATION

Corresponding Author
*E-mail emilio.nunez@usc.es.

■ ACKNOWLEDGMENT

The authors thank "Centro de Supercomputación de Galicia" (CESGA) for the use of their computational devices. S.A.V. and E.M.-N. thank "Xunta de Galicia" for financial support ("Axuda para a Consolidación e Estructuración de unidades de investigación competitivas do Sistema Universitario de Galicia, 2007/50, cofinanciada polo FEDER 2007-2013"). Z.H. acknowledges financial support from the Ministry of Science, Research and Technology of Iran.

■ REFERENCES

(1) Tarrazo-Antelo, T.; Martinez-Nunez, E.; Vazquez, S. A. *Chem. Phys. Lett.* **2007**, *435*, 176.
(2) Martinez-Nunez, E.; Vazquez, S. *Chem. Phys. Lett.* **2006**, *425*, 22.
(3) Martinez-Nunez, E.; Vazquez, S. *J. Chem. Phys.* **2005**, 122.
(4) Martinez-Nunez, E.; Vazquez, S. A.; Aoiz, F. J.; Banares, L.; Castillo, J. F. *Chem. Phys. Lett.* **2004**, *386*, 225.
(5) Martinez-Nunez, E.; Vazquez, S. *J. Chem. Phys.* **2004**, *121*, 5179.
(6) Gonzalez-Vazquez, J.; Martinez-Nunez, E.; Fernandez-Ramos, A.; Vazquez, S. A. *J. Phys. Chem. A* **2003**, *107*, 1398.
(7) Gonzalez-Vazquez, J.; Fernandez-Ramos, A.; Martinez-Nunez, E.; Vazquez, S. A. *J. Phys. Chem. A* **2003**, *107*, 1389.
(8) Martinez-Nunez, E.; Estevez, C. M.; Flores, J. R.; Vazquez, S. A. *Chem. Phys. Lett.* **2001**, *348*, 81.
(9) Martinez-Nunez, E.; Vazquez, S. A. *Chem. Phys. Lett.* **2000**, *332*, 583.
(10) Jalenak, W. A.; Nogar, N. S. *J. Chem. Phys.* **1983**, *79*, 816.
(11) Umemoto, M.; Seki, K.; Shinohara, H.; Nagashima, U.; Nishi, N.; Kinoshita, M.; Shimada, R. *J. Chem. Phys.* **1985**, *83*, 1657.
(12) Fletcher, T. R.; Leone, S. R. *J. Chem. Phys.* **1988**, *88*, 4720.
(13) Huang, Y.; Yang, Y.; He, G.; Hashimoto, S.; Gordon, R. J. *J. Chem. Phys.* **1995**, *103*, 5476.
(14) He, G.; Yang, Y.; Huang, Y.; Hashimoto, S.; Gordon, R. J. *J. Chem. Phys.* **1995**, *103*, 5488.
(15) Blank, D. A.; Weizhong, S.; Suits, A. G.; Lee, Y. T.; North, S. W.; Hall, G. E. *J. Chem. Phys.* **1998**, *108*, 5414.
(16) Lee, Y. R.; Wang, L. D.; Lee, Y. T.; Lin, S. M. *J. Chem. Phys.* **2000**, *113*, 5331.
(17) Lin, S. R.; Lin, S. C.; Lee, Y. C.; Chou, Y. C.; Chen, I. C.; Lee, Y. P. *J. Chem. Phys.* **2001**, *114*, 160.
(18) Lin, S. R.; Lin, S. C.; Lee, Y. C.; Chou, Y. C.; Chen, I. C.; Lee, Y. P. *J. Chem. Phys.* **2001**, *114*, 7396.
(19) Ko, H. S.; Lee, Y. R.; Chen, C. C.; Wang, L. D.; Lin, S. M. *J. Chem. Phys.* **2002**, *117*, 6038.
(20) Bahou, M.; Lee, Y. P. *Aust. J. Chem.* **2004**, *57*, 1161.
(21) Riehl, J.-F.; Morokuma, K. *J. Chem. Phys.* **1994**, *100*, 8976.
(22) Kato, S.; Morokuma, K. *J. Chem. Phys.* **1981**, *74*, 6285.
(23) Takayanagi, T.; Yokoyama, A. *Bull. Chem. Soc. Jpn.* **1995**, *68*, 245.

(24) Abrash, S. A.; Zehner, R. W.; Mains, G. J.; Raff, L. M. *J. Phys. Chem.* **1995**, *99*, 2959.
(25) Barbatti, M.; Aquino, A. J. A.; Lischka, H. *J. Phys. Chem. A* **2005**, *109*, 5168.
(26) Blank, D. A.; Suits, A. G.; Lee, Y. T.; North, S. W.; Hall, G. E. *J. Chem. Phys.* **1998**, *108*, 5784.
(27) North, S. W.; Hall, G. E. *Chem. Phys. Lett.* **1996**, *263*, 143.
(28) Bird, C. A.; Donaldson, D. J. *Chem. Phys. Lett.* **1996**, *249*, 40.
(29) Fahr, A.; Laufer, A. H. *J. Phys. Chem.* **1992**, *96*, 4217.
(30) Derecskei-Kovacs, A.; North, S. W. *J. Chem. Phys.* **1999**, *110*, 2862.
(31) Letendre, L.; Dai, H.-L. *J. Phys. Chem. A* **2002**, *106*, 12035.
(32) Wilhelm, M. J.; Nikow, M.; Letendre, L.; Dai, H.-L. *J. Chem. Phys.* **2009**, *130*, 044307.
(33) Gonzalez, C.; Schlegel, H. B. *J. Phys. Chem.* **1990**, *94*, 5523.
(34) Frisch, M. J.; Trucks, G. W.; Schlegel, H. B.; Scuseria, G. E.; Robb, M. A.; Cheeseman, J. R.; Scalmani, G.; Barone, V.; Mennucci, B.; Petersson, G. A.; Nakatsuji, H.; Caricato, M.; Li, X.; Hratchian, H. P.; Izmaylov, A. F.; Bloino, J.; Zheng, G.; Sonnenberg, J. L.; Hada, M.; Ehara, M.; Toyota, K.; Fukuda, R.; Hasegawa, J.; Ishida, M.; Nakajima, T.; Honda, Y.; Kitao, O.; Nakai, H.; Vreven, T.; Montgomery, J., J. A.; ; Peralta, J. E.; Ogliaro, F.; Bearpark, M.; Heyd, J. J.; Brothers, E.; Kudin, K. N.; Staroverov, V. N.; Kobayashi, R.; Normand, J.; Raghavachari, K.; Rendell, A.; Burant, J. C.; Iyengar, S. S.; Tomasi, J.; Cossi, M.; Rega, N.; Millam, N. J.; Klene, M.; Knox, J. E.; Cross, J. B.; Bakken, V.; Adamo, C.; Jaramillo, J.; Gomperts, R.; Stratmann, R. E.; Yazyev, O.; Austin, A. J.; Cammi, R.; Pomelli, C.; Ochterski, J. W.; Martin, R. L.; Morokuma, K.; Zakrzewski, V. G.; Voth, G. A.; Salvador, P.; Dannenberg, J. J.; Dapprich, S.; Daniels, A. D.; Farkas, Ö.; Foresman, J. B.; Ortiz, J. V.; Cioslowski, J.; Fox, D. J. *Gaussian 09*, revision A.02; Gaussian Inc.: Wallingford, CT, 2009.
(35) Miller, W. H. *J. Am. Chem. Soc.* **1979**, *101*, 6810.
(36) Bortz, A. B.; Kalos, M. H.; Lebowitz, J. L. *J. Comput. Phys.* **1975**, *17*, 10.
(37) Gillespie, D. T. *J. Comput. Phys.* **1976**, *22*, 403.
(38) Ervin, K. M.; Ho, J.; Lineberger, W. C. *J. Chem. Phys.* **1989**, *91*, 5974.
(39) Moffat, J. B. *J. Phys. Chem.* **1977**, *81*, 82.